machine tool, parallel kinematics,
simulation, active damping

Markus WABNER*
Sebastian GRZEJSZCZYK**
Reimund NEUGEBAUER*,**

POTENTIAL OF MANIPULATING THE DAMPING PROPERTIES OF PARALLEL KINEMATIC MACHINE TOOLS

Parallel kinematics with a higher end-effector degree of freedom such as hexapods and pentapods consist of a large number of joints and slender struts. However, it is only possible to create comparably low levels of bearing and strut bending stiffness at reasonable expense due to the limited construction space. That means that these structures are very susceptible to vibration. Even in the low-frequency range they have a large number of relevant eigenmodes that are only dampened slightly. Simultaneously, it is difficult to analyze vibrational properties due to coupled eigenmodes, which also makes it difficult to discover ways to remedy this situation. This article will take the example of a pentapod to analyze the dynamic properties of slightly dampened parallel kinematics by simulation to study potential means of manipulating it. This will include a description of the model formation of the mechanical system. The article will also address ways of reducing model size and using various simulation environments to boost analysis efficiency. Finally, both passive and active strategies will be studied and evaluated for boosting damping. Amongst others it could be shown that it is not necessary to damp every of the five kinematic chains to achieve effective improvement of the system damping behaviour.

1. INTRODUCTION

Pentapod and hexapod structures consist of 5 or 6 kinematic chains linked to one another. These chains are generally formed of one strut, the corresponding number of joints and an feed drive. It is necessary to set up the joints in a very tight space and design struts as slim as possible to generate the best kinematic properties and high axis dynamics. The joints are best formed of pretensible combinations of roller bearings that only dampen slightly. These design constraints mean that the joints are much less rigid than the guide systems for serial machine structures, and the struts only have slight flexural strength. This results in higher vibration susceptibility with simultaneously limited system damping. At the same time, its vibration properties are substantially more complex and therefore more difficult to capture due to the coupled kinematic chains, the large number of discrete elasticity points and the greater position dependencies of properties.

* Fraunhofer Institute for Machine Tools and Forming Technology IWU, Chemnitz
** Institute of Machine Tools and Manufacturing Processes, Technical University of Chemnitz

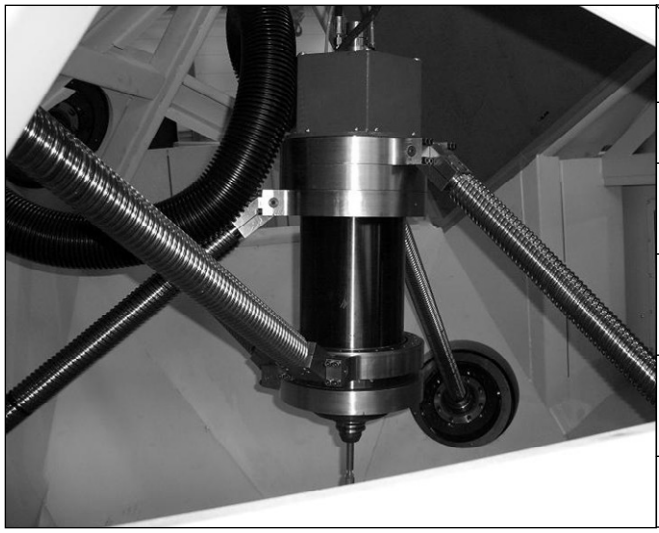

Chains \ DOF.	2	3	4	5	6
2	8 (4,4/3,5/2,6)	9 (4,5/3,6)	10 (5,5/4,6)	11 (5,6)	12 (6,6)
3	14 (4,5,5/2,6,6/ 4,4,6/3,5,6)	15 (5,5,5/4,5,6 3,6,6)	16 (5,5,6/4,6,6)	17 (5,6,6)	18 (6,6,6)
4	20 (5,5,5,5/4,5,5,6/ 3,5,6,6/4,4,6,6)	21 (5,5,5,6/4,5,6,6 3,6,6, 6)	22 (5,5,6,6/ 4,6,6,6)	23 (5,6,6,6)	24 (6,6,6,6)
5	26 (5,5,5,5,6 4,5,5,6,6)	27 (5,5,5,6,6/ 4,5,6,6,6)	28 (5,5,6,6,6/ 4,6,6,6,6)	29 (5,6,6,6,6)	30 (6,6,6,6,6)
6	32 (5,5,5,5,6,6)	33 (5,5,5,6,6,6)	34 (5,5,6,6,6,6)	35 (5,6,6,6,6,6)	36 (6,6,6,6,6,6)

Fig. 1: Working platform of the pentapod machine tool (left) and the systematics of PKM structures [7] (right) with the number of DOF of each kinematic chain (marked field: pentapod)

This article will take the example of a machine tool with a pentapod structure (Fig. 1) to demonstrate an option for simulating vibration properties of parallel kinematics (PKM) for discovering where they can be manipulated for reducing dominant resonance ratios. Its system properties are described based upon the finite elements method (FEM) and subsequent tests will be carried out in the MATLAB/SIMULINK software environment because it significantly minimizes calculating times and can include controlled drives. The first part of this article will apply the tools of vibration cause analysis, model size reduction and implementing physical models in the SIMULINK environment on the pentapod. It will then study the influence of damping variation of specific subassemblies on vibration properties on the frequency response function (FRF). The last part will discuss how to trandfer this potential for improvement into real life.

2. MODELING

2.1. GENERAL WORKFLOW

Machine tools are conventionally analyzed with multibody analysis (MBA) or FEM. There are drawbacks to MBA in mapping the elastic properties of complex mechanical structures and higher-order vibration modes, although it is effective in terms of computing times, simulating travel movements and because it can include drives and control systems. Although vibration properties of complex mechanical components can be mapped much better with FEM than MBA, it still has the drawback of high computing time intensity with dynamic analyses. In other words, extensive analyses with a large number of parameters variations could take an extremely long period of time. Beyond this, it is hardly possible to include major travel movements and controlled drives. If major travel movements are not necessary, then this can be a good combination of the benefits of FEM and MBA, particu-

larly with the state space (SS) representation used in control engineering. SS representation is a mathematical model of a physical system as a set of input, output and state variables related by first-order differential equations and can be used in SIMULINK. The SS representation used in this article is

$$\begin{aligned} \dot{x} &= Ax + Bu \\ y &= Cx + Du \end{aligned} \tag{1}$$

A system (matrix)
B input (matrix)
C output (matrix)
D direct transmission (matrix)
u input (scalar)
x state of the system (column vector)

The theoretical interactions are described in [5] and the following items allow a rough description of how to create the SS model of the pentapod:

1. generating coupled equations of motion and initial conditions in the FEM environment
2. calculating eigenvalues and eigenvectors in the FEM environment
3. model size reduction
4. generating the SS matrices *A, B, C and D*

The following will address the FEM model and model size reduction in greater detail.

2.2. EIGENVALUE PROBLEM AND CAUSES OF VIBRATION

The pentapod model is created and modal parameters are simulated with FEM. This parametric model consists of 150,000 nodes while possessing 800,000 degrees of node freedom (DOF) (Fig. 2). Since it is not necessary to include damping to create the SS model, the only thing that has to be applied is the rigidity and mass matrix including their respective constraints with special consideration of the machine position where the eigenvalue problem has to be solved for each machine position of interest. The first 500 eigenvalues occur in a frequency range of as much as 750 Hz and Fig. 5 (above) can be used to assess the distribution of the eigenmodes via frequency. Manipulating the vibration properties necessitates identifying the subassemblies that cause the eigenfrequencies. It is hardly possible to analysis the causes of the PKM types by simply observing the FEM vibration form plots or animations because rigid body movements and elastic deformations generally overlap with PKM. Or, to put it differently: PKM vibrations cause kinematic movements in the working platform (WP) particularly in the low-frequency range. In turn, this often generates rotating rigid body movements in the struts and WP, although they should not be deemed the cause of the vibration. The kinematic proportion of the vibration may be greater than the actual

cause of the vibration, which makes it substantially more difficult to identify the causes of the vibration while easily leading to incorrect interpretations.

A method has been applied according to Neuber [4] to at least approximately identify the causes of the vibration. This method can be used to assess the lowest eigenfrequency of multiple-mass oscillators, although it also delivers approximate statements on the impact specific elasticities have on the level of eigenfrequencies. This method was applied by neglecting all elasticities during an FEM modal analysis ensuring that only the elasticity to be studied (such as the joints or struts) stays elastic.

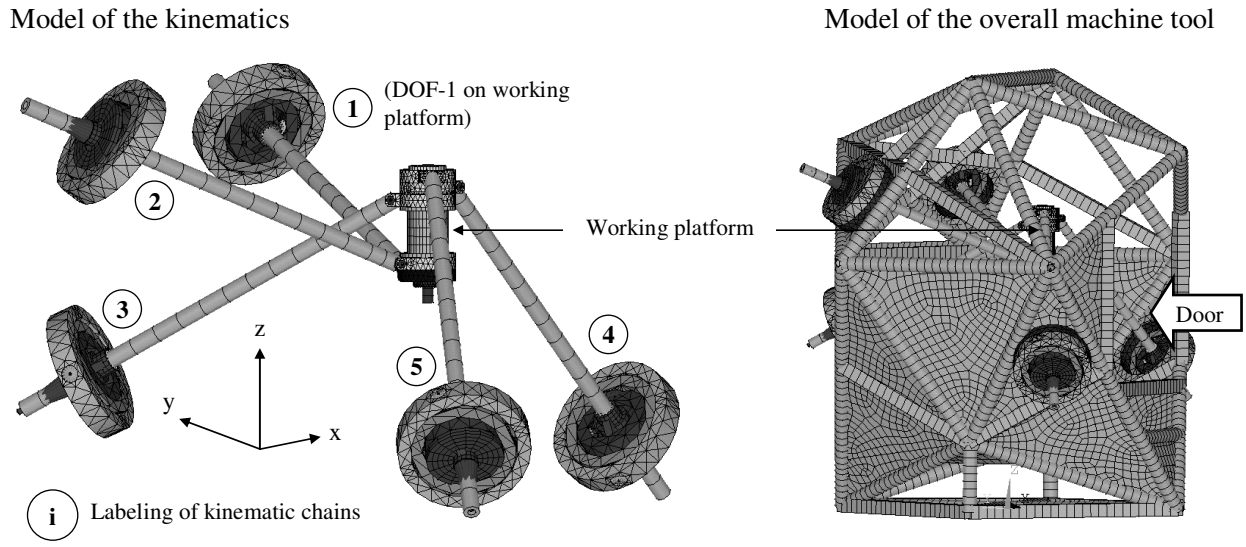

Fig. 2: FEM model and labeling the kinematic chains of the machine tool analyzed

The analysis found that it is possible to assess the impact that the frame, struts and joints on the WP and basis platform (BP) had on specific eigenfrequencies (also see Fig. 6 above). It is not only the first frame vibration, but also the first bending eigenforms of the struts that are responsible for the lowest eigenfrequencies. Afterwards, the joint elasticities on the BP caused the axial vibrations on the struts whereas there are other bending modes on the struts and local frame vibrations in the higher-frequency range.

2.3. MODEL SIZE REDUCTION

The degree of freedom of the FEM model and the number of modes should be reduced before creating the SS model. Fig. 3 shows one way to do this. First of all, FEM is used to carry out a modal analysis of the undamped system to calculate the eigenvalue vector ω (Block Lanczos is a FEM solver suited to models of this size). The next two steps are selecting the nodes pertinent to downstream analyses and the appropriate DOF while creating the normalized modal matrix z_n for them. Incidentally, the SS model can be created according to [5] based upon the eigenfrequency vector ω and normalized modal matrix z_n, although this will not be described in greater detail here.

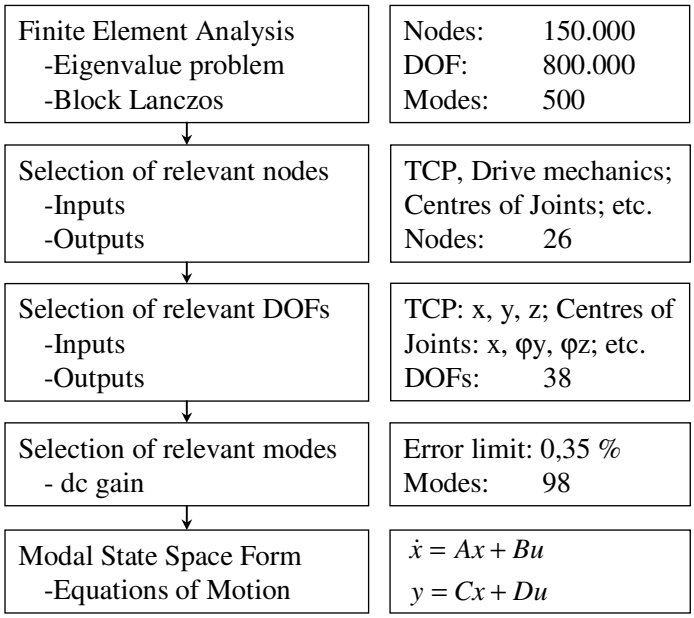

Fig. 3: Model size reduction flowchart according to [2] and application

The model size can be substantially reduced again if only eigenmodes are applied that are significant to the DOF selected. A case in point is local frame vibrations, a lot of which do not have any impact on the tool center point (TCP) or strut vibrations. Calculating the static reinforcement *dc* gain can produce a systematic analysis of the relevance of specific eigenmodes $i = 1 .. m$ for the DOF selected for the machine [2]. The general formula for equally modally dampened systems ($\zeta_i = \zeta = const.$ [%] of critical damping) and an undamped system is:

$$\frac{z_j}{F_k} = \sum_{i=1}^{m} \frac{z_{nji} z_{nki}}{s^2 + \omega_i^2} \tag{2}$$

$$\frac{z_j}{F_k} = \sum_{i=1}^{m} \frac{z_{nji} z_{nki}}{s^2 + 2\zeta_i \omega_i s + \omega_i^2} \tag{3}$$

F_k is the force applied at DOF k and z_j is the displacement taken at DOF j.

This formula indicates that in general each transfer function consists of the total of the systems of one degree of freedom. Each system is determined by each input/output eigenvector z_{nji}, z_{nki} and the eigenvalue ω_i. If we substitute $s = j\omega = j0 = 0$, we get the frequency response at dc, the dc gain for the i^{ten} eigenmode. This is the same for the dampened and undamped case:

$$\frac{z_{ji}}{F_{ki}} = \frac{z_{nji} z_{nki}}{\omega_i^2} = dc_{ijk} \tag{4}$$

It can be proven for resonancy that the ratios of *dc* gain to be calculated according to the formula above also apply to equally modally dampened systems, although this will not be described in greater detail here. The greater *dc(i)* is, the greater is the impact of the ith eigenvalue. If *dc(i)* is small enough, its eigenmode can be neglected and omitted from the modal matrix.

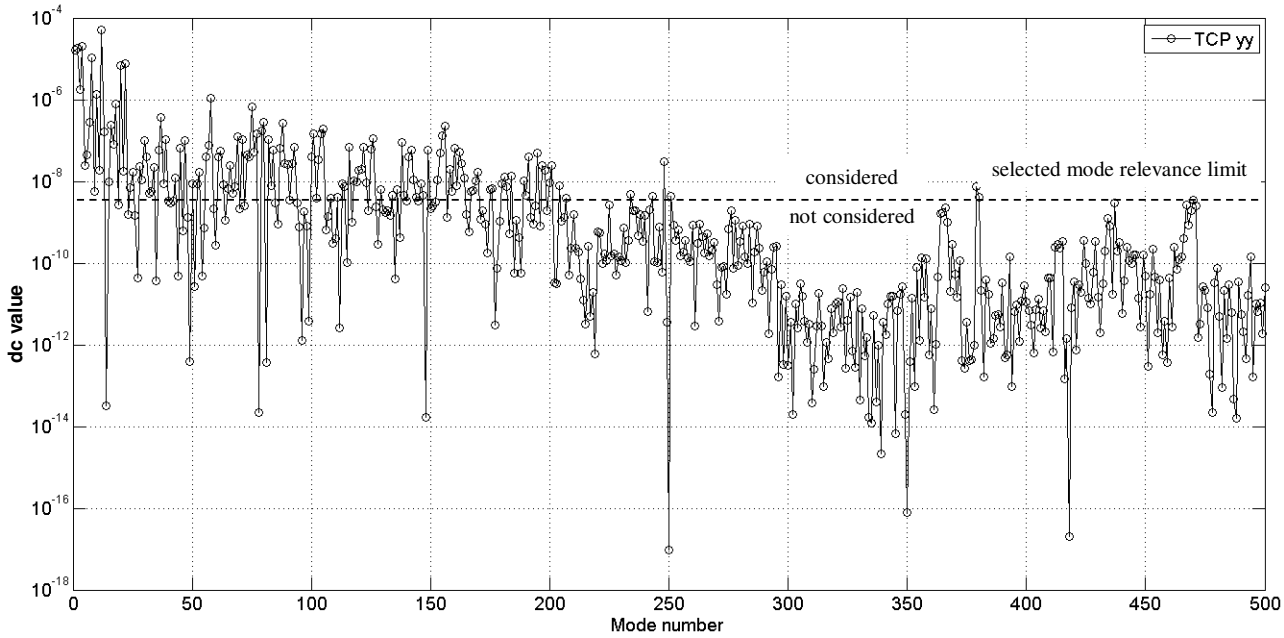

Fig. 4: Dc value of each mode for input/output TCP yy

Figure 4 shows an example of *dc* gain for input (TCP y) and output (TCP y) and 98 of the altogether 500 modes are included at a relevance limit of $5 \cdot 10^{-8}$. The percentage error resulting in comparison to the original model from mode reduction at $\Omega = 0$ can be calculated with

$$dc_{jk}(\Omega = 0) = \frac{G_{red} - G}{G} \cdot 100\% \tag{5}$$

The error in including 98 modes is approximately 0.32% for TCP yy. However, mode evaluation via *dc* gain is no longer correct if each eigenmode is separately dampened, and the gain at the point of resonancy has to be used instead. The subsequent basic simulations will forego adjusting the damping properties for measurements while assuming a constant value $\zeta_i = \zeta = 0.1\%$ of critical damping for all eigenmodes. Then, the SS model is created based upon the mode reduction and damping described, which would mean that the images below do not reflect the eigenvectors of the actual machine (modal damping for the actual machine is 2–12 times larger if the eigenmode is dominant).

3. VIBRATIONAL PROPERTIES OF THE MACHINE TOOL

Fig. 5 and 6 show the simulated FRF of the original scenario of the pentapod on the assumed TCP for two machine positions in the frequency range bin 400 Hertz (ISO units are used in the absence of other specifications). Fig. 5 also has the distribution of the eigenmode numbers to point out once again to the importance of mode reduction. In addition, Fig. 6 also shows the relevant causes of the vibration. The position and directional dependencies of the machine properties can be easily seen in these pictures and the directional dependency is particularly strong at the P2 edge position. Furthermore, the first frame eigenmode can also be seen at 27 Hz in the x-direction and the second dominant frame eigenmode at 67 Hz in the vertical direction. Both modes are essentially caused by the installation conditions of the machine, although in reality they are substantially more dampened. Other eigenmodes typical for PKM are caused by the bending vibrations of the struts and the elasticities of the joints, particularly the BP joints. These are the eigenmodes that are also dominant on the actual machine. What is interesting here is the fact that the bending eigenmodes are actually pertinent to the WP, although the "reaction forces" of the struts do not exert a force in the feed direction with bending vibrations. In other words, they can only impact the WP position indirectly.

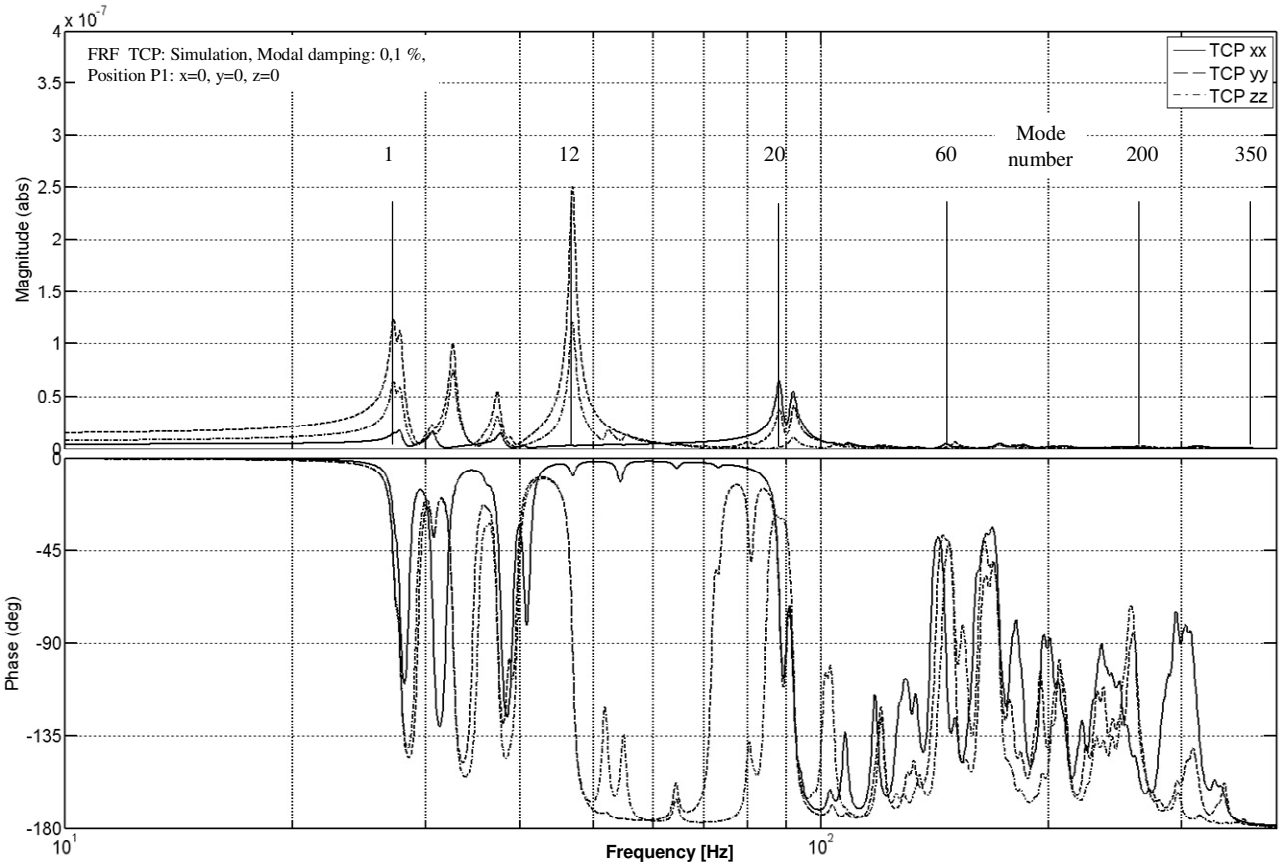

Fig. 5: FRF at TCP and position P1

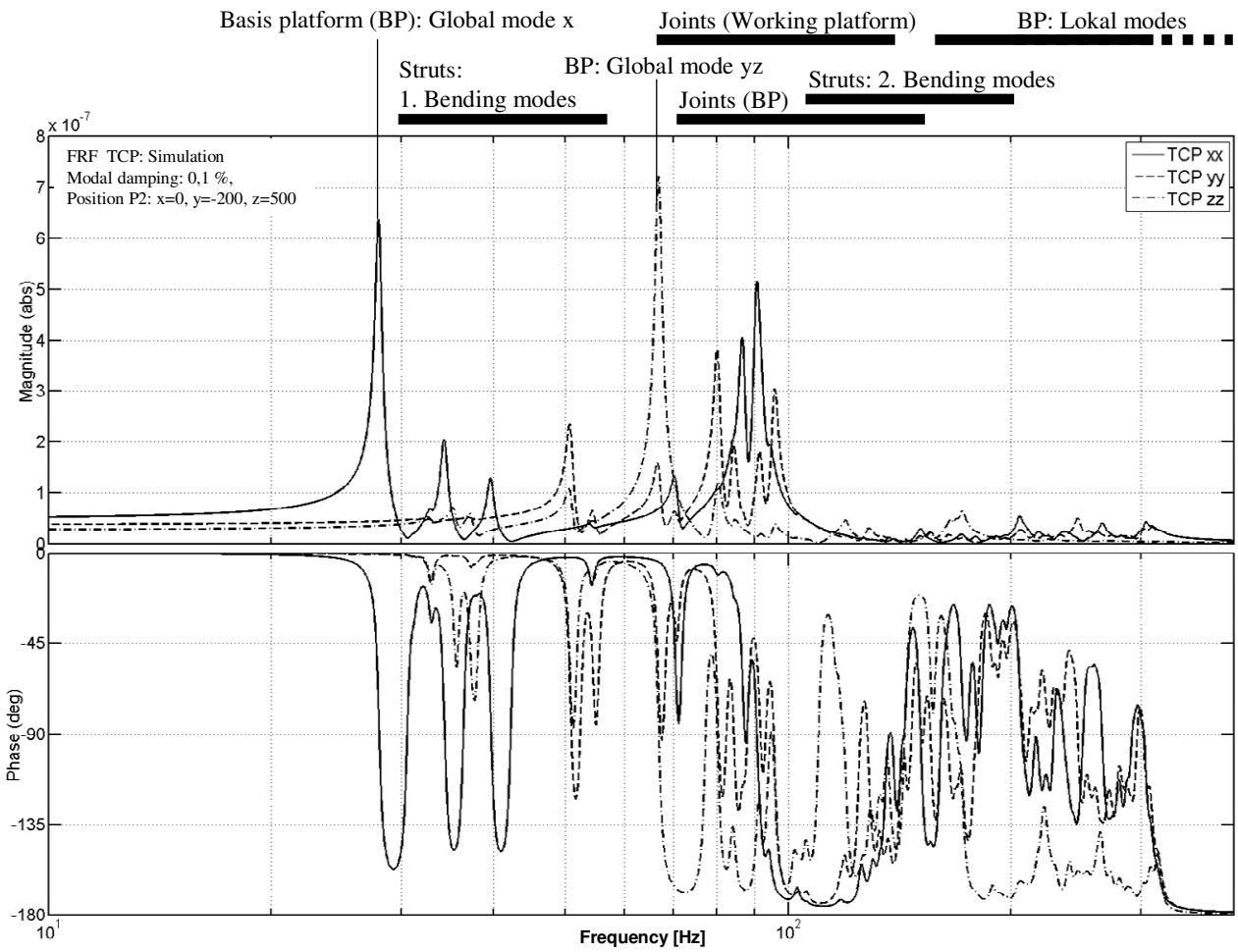

Fig. 6: FRF at TCP and position P2

4. LOCAL VELOCITY FEEDBACK DAMPING

The sensitive analyses below calculate the impacts that a discrete increase in damping for specific subassemblies has on the system properties on the TCP primarily focusing on the necessary damping locations. The discrete dampers are modeled with a damping force F_d or damping moment M_d that is viscous or proportional to speed:

$$F_d = b_L \cdot \frac{dx}{dt} \qquad\qquad M_d = b_B \cdot \frac{d\varphi}{dt} \tag{6}$$

Studies are made in the first step regardless of whether the damping values selected can actually be brought about with practical solutions. The second step places the knowledge gained alongside specific options for technically building them, although the latter will not be the subject matter of this paper.

As noted above, the bending vibrations of the first eigenform of the struts cause the dominant resonance ratios in the lower frequency range. Generally two first bending eigenforms occur per strut due to the design of the strut joints that are vertical to one another and differ by 5-20 Hz from one another. The rotations of the strut nodes can be used in the first approximation both for detecting strut vibrations and conducting damping forces. Fig. 7 uses the rotations of the two nodes on the ends of the struts while the first bending eigenform can be detected or rigid body modes can be rejected by forming the difference. Other nodes have to be taken into consideration to reliably map the second bending eigenmodes. Frequency-dependent filters can be used to separately analyze different modes. However, since the second bending eigenmodes are only of subordinate relevance on the actual machine and the model, model formation will not be described in greater detail here.

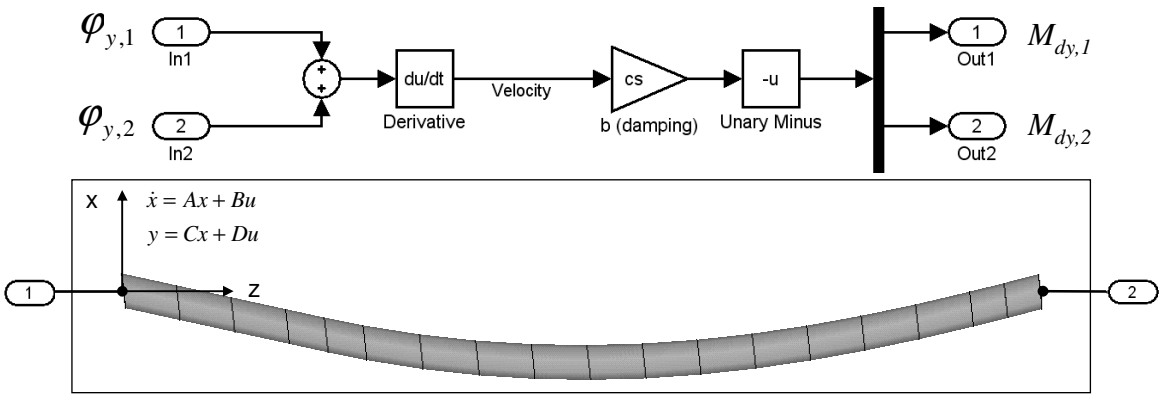

Fig. 7: Modeling of viscous damping for the first bending mode of a strut

Boosting the damping of the bending eigenmodes reduces the resonance ratios in the lower frequency range. What is peculiar here is the fact that this dampens the first frame eigenmode. The resonance ratios disappear almost completely if all struts are dampened at b = 20,000 Ns/m and the strut vibrations have a measurable impact on system properties even if b is very great and cannot be achieved with material damping. Fig. 8 shows the effect that great strut damping has on the FRF on the TCP x, position P2. It became apparent during tests that that each of the struts has a varied degree of relevance for the vibration properties of the TCP. Greater damping on struts 1 and 2 (refer to Fig. 2 for the designation) has a significant impact regardless of the machine position and direction of excitation under study. The reason for this is the fact that the two WP strut joints are closer to the TCP. It can be seen in Fig. 8 that great damping for the two struts in position P2 has virtually the same impact on the FRF as damping all struts. The extent that the struts contribute to overall damping increase is never below 70% at other machine positions.

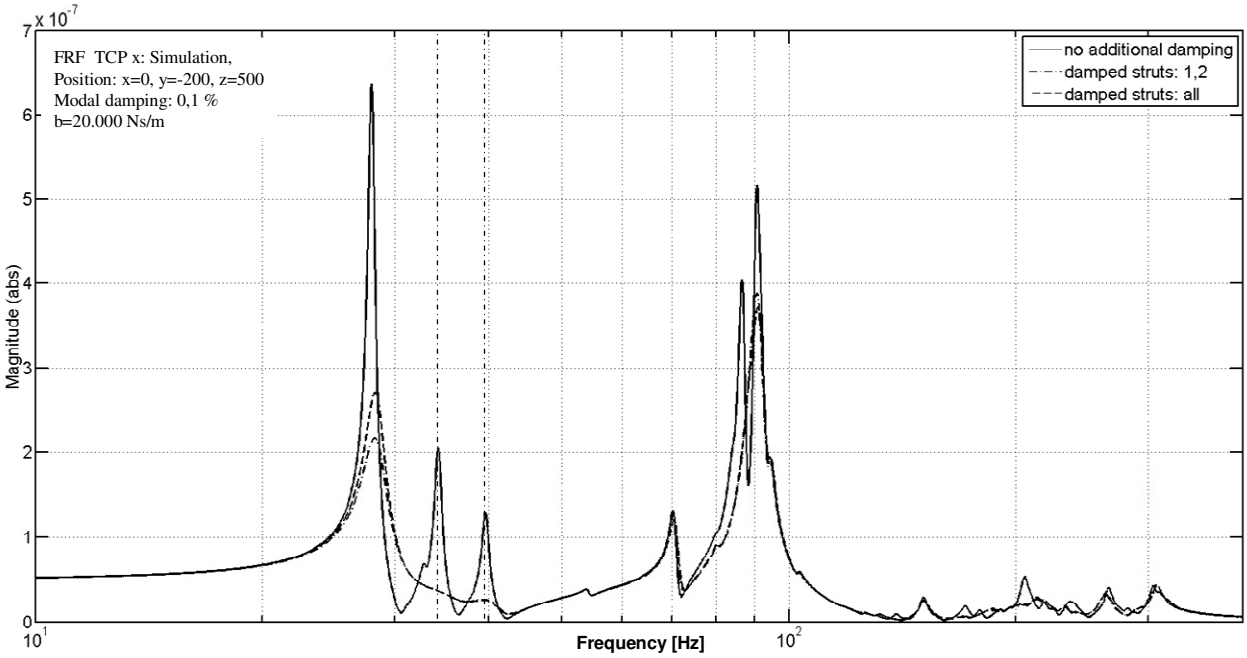

Fig. 8: Viscous damping of strut bending modes (TCP x, Position P2)

4.2. AXIAL VIBRATIONS OF THE STRUTS CAUSED BY JOINTS OF THE BASIS PLATFORM

The elasticity of the cardan joints (configured from radial needle roller bearings) on the base platform causes rigid body modes for the struts in the axial direction (feed direction) that cause significant resonance ratios on the TCP in the range between 70 Hz and 110 Hz. Boosting the damping in the cardan joints can effectively reduce the resonance ratios. The

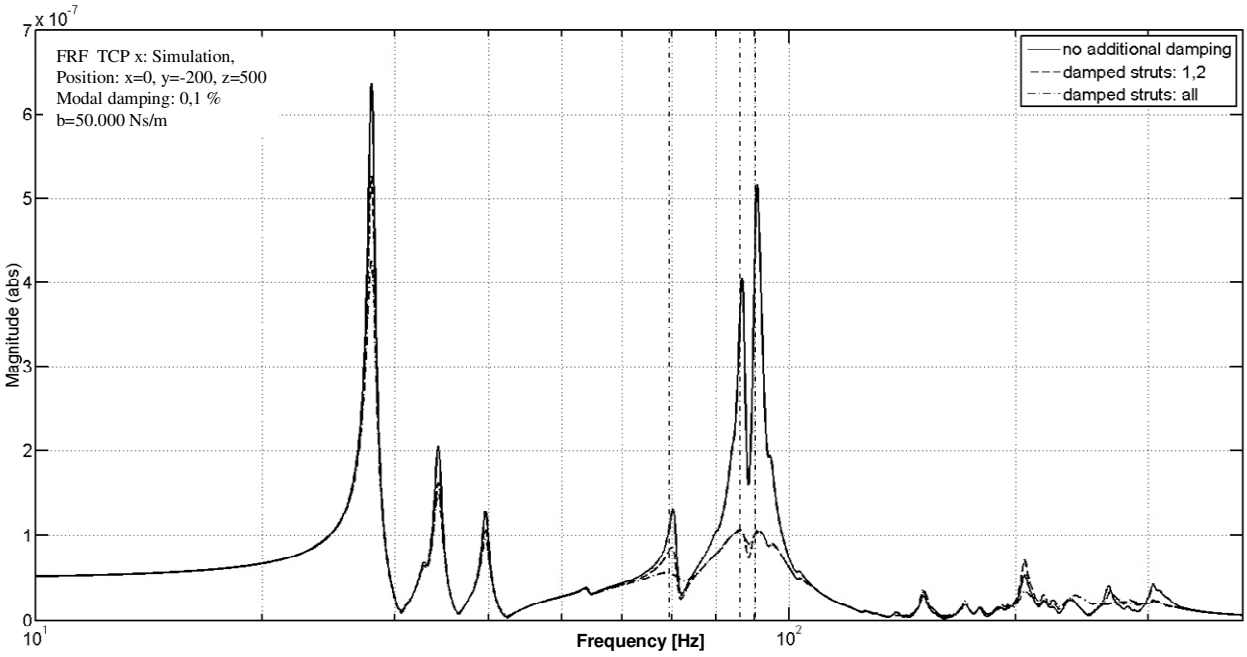

Fig. 9: Viscous damping of axial strut modes (TCP x, Position P2)

additional damping is modeled by including a damper between the strut and outside cardan ring fastened to the machine frame. Struts 1 and 2 have made dominant contribution to overall axial damping in an analogous fashion to bending vibrations. The high level of relevance of the two struts is also mostly independent of machine position and direction of excitation. Fig. 9 shows the theoretical impact that discrete damping of axial vibrations of b = 50,000 Ns/m has on the FRF TCP x, position P2.

4.3. VIBRATIONS OF THE WORKING PLATFORM

Damping forces on the TCP were conducted into the working platform to study what impact an increase in damping would have in the area of the process point. In this case, damping does not have a relative impact between the machine subassemblies, but an absolute impact in the global coordinate system. This type of damping could be brought about by proof mass actuators (PMA) such as [3][8][6]. They also have the benefit of reaching a broadband impact regardless of the subassemblies causing the vibration. Fig. 10 shows the impact of added viscous damping of b = 20,000 Ns/m on the FRF on the TCP x, position P2.

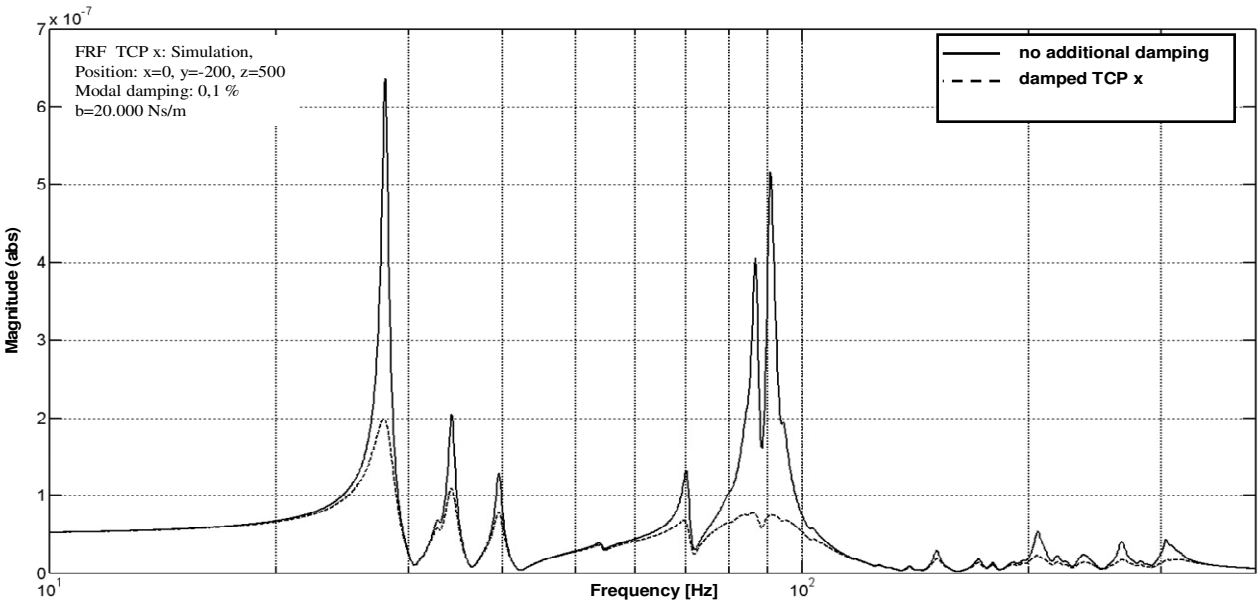

Fig. 10: Viscous damping of TCP vibrations relative to a global normal (TCP x, Position P2)

4.4. DEFINING AN ACTIVE DAMPER

The degrees of damping presented in chapters 4.1.–4.3. cannot be brought about with a passive design (material damping or damping in the joints) or only with a great deal of time and expenditure. In contrast, added active systems can deliver the needed degrees of damping. One benefit of the MATLAB/SIMULINK simulation environment used is the fact that it can trace the technical requirements made of added active systems without a great deal of time effort.

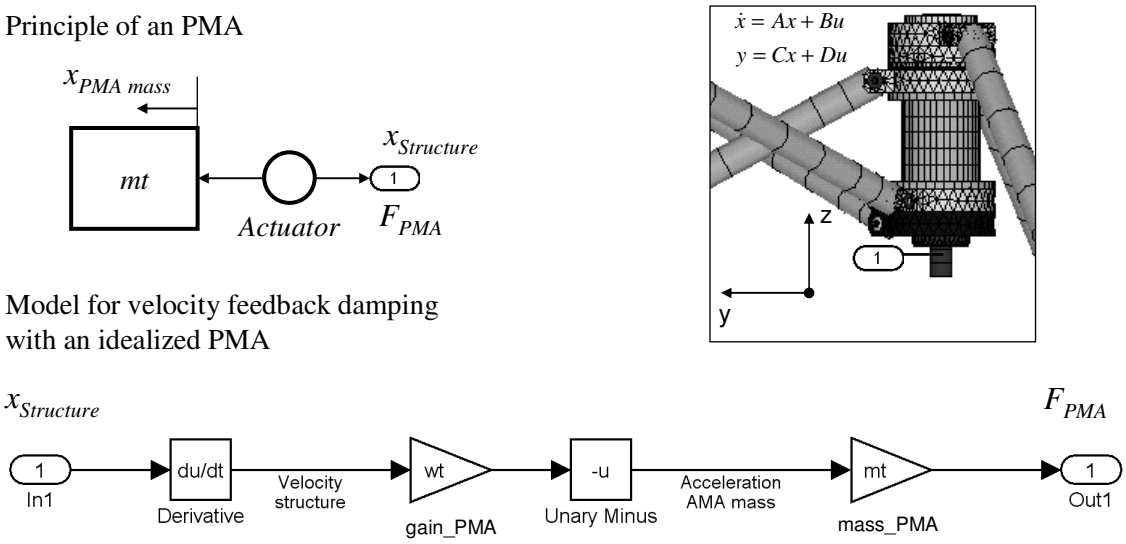

Fig. 11: Principle and model of an idealized proof mass actuator for viscous damping

Fig. 11 shows the principle and a simplified simulation structure for a proof mass actuator (PMA). Newton's Second Axiom states that the active mass of the PMA has to be accelerated proportional to the vibrational speed of the structure to be dampened to generate viscous damping force. That means that it is possible to calculate the reaction mass and stroke needed for a specified degree of damping. EHMANN [1] derives these interrelations for a selected eigenfrequency by analytical means while Fig. 12 shows the necessary amplitudes of damper force and mass path to generate the viscous damping shown in Fig. 10 for two ideal PMA including an harmonic excitation of the machine on the TCP x of ±10 N. This simulation environment makes it possible to calculate the interrelation between the desired

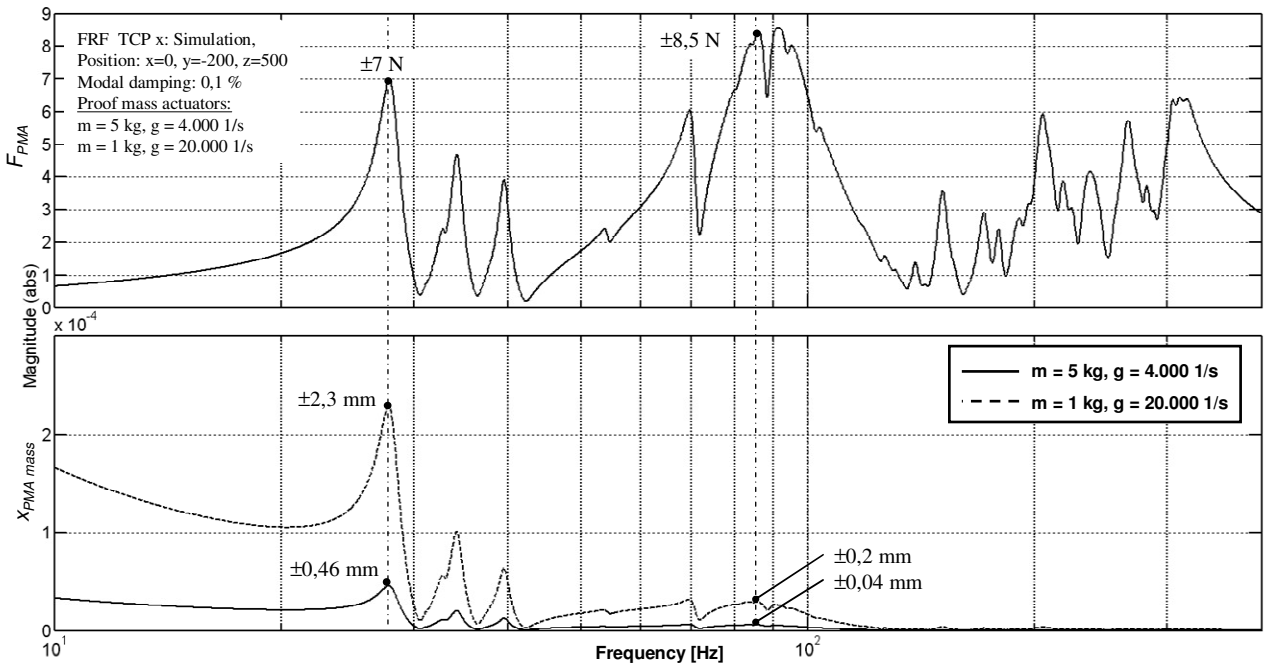

Fig. 12: Necessary damping force amplitudes and strokes of PMA mass for generating the viscous damping properties shown in Fig. 10

damper force and needed stroke for the entire frequency range. For instance, a reaction mass of 5 kg was selected in Fig. 12 for the first damper to generate the required gain of 4,000 1/s and maximum stroke of ±0.46 mm. The second damper configuration has a reaction mass of 1 kg, maximum stroke of ±2.3 mm and a gain of 20,000 1/s. Finally, the impulse response function of the PMA is shown analogously in Fig. 13 where it can be seen that an actual damping system requires much more complex control with filters since very low-frequency vibrations theoretically add up to very high amplitudes for the PMA mass.

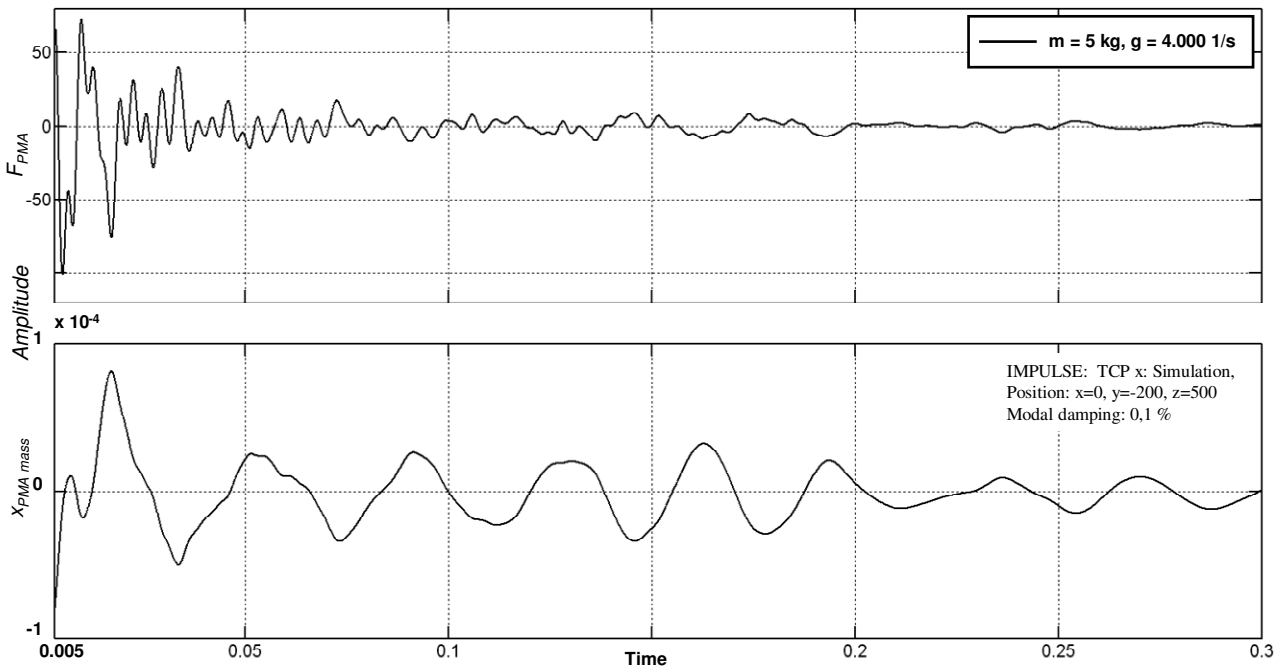

Fig. 13: Step response function of an proof mass damper for generating the viscous damping properties shown in Fig. 10

5. CONCLUSIONS

First of all, this article took the example of a machine tool with a pentapod structure to simulate and analyze the vibration properties of parallel kinematics. It identified the subassemblies causing the vibration properties and applied sensitive analyses to study the impact of added discrete dampers. This bore out the thesis that the low flexural strength of the struts and low joint elasticities were the main reason for the most dominant resonance ratios. Secondly, this article showed that not all kinematic chains are equally important to the TCP vibration properties. The simulation environment used – a combination of the finite elements method and MATLAB/SIMULINK – proved to be excellently suited to this study in connection with extensive model size reduction. The minimum simulation periods achieved allow a whole series of parameter variations while being excellent for streamlining work. Both complex mechanical structures and controlled drives can be included here. That means that mechatronic systems can be easily simulated if they do not have to make great move-

ments. A simple example was used to demonstrate this principle of deducing the requirements made of a proof mass actuator for generating viscous damping forces. Admittedly, there is still a lot of work to be done to correctly map the actual damping properties of machine tools. However, to show basic effects only, the model was not mapped to experimental examined modal damping. In any event, the model will have to be adapted to have a quantitative description of damping properties.

REFERENCES

[1] EHMANN, C., NORDMANN, R., *Low Cost Actuator for Active Damping of Large Machines*, Conf.-Speech, Mechatronics Conf., Berkeley, California, 2002.

[2] HATCH, M. R., *Vibration Simulation Using Matlab and ANSYS*, Chapman and Hall/CRC, Boca Raton, FL, 2000.

[3] MAY, C., PAGLIARULO, P., JANOCHA, H., *Optimisation of a Magnetostrictive Auxiliary Mass Damper*, Actuator 2006, Proc. 10th Int. Conf. on New Actuators, 2006, pp. 344-348.

[4] NEUBER, H., *Über allgemeine Eigenschaften der Schwingungszahlen linear-elastischer Systeme*, Archive of Applied Mechanics, 1959, 28/1, pp. 229-241.

[5] SONTAG, E. D., *Mathematical Control Theory: Deterministic Finite Dimensional Systems*, Second Edition, Springer, 1999.

[6] WECK, M., SCHULZ, A., *Active Auxiliary Mass Damper*, Production Engineering, 2004, XI/1, pp. 39-43.

[7] WEIDERMANN, F., *Strukturoptimierung von parallelkinematischen Werkzeugmaschinen*, PhD Thesis, TU Chemnitz, 2001.

[8] www.micromega-dynamics.com